Magnetic penetration depth in single crystals of $SrPd_2Ge_2$ superconductor

H. Kim,[1,*] N. H. Sung,[2,†] B. K. Cho,[2,3,‡] M. A. Tanatar,[1,§] and R. Prozorov[1,|]

[1]*The Ames Laboratory and Department of Physics and Astronomy, Iowa State University, Ames, Iowa 50011, USA*

[2]*School of Materials Science and Engineering, Gwangju Institute of Science and Technology (GIST), Gwangju 500-712, Korea*

[3]*Department of Photonics and Applied Physics, Gwangju Institute of Science and Technology (GIST), Gwangju 500-712, Korea*

(Received 25 January 2013; revised manuscript received 28 February 2013; published 19 March 2013)

The in-plane magnetic penetration depth $\lambda_m(T)$ was measured in a single crystal of $SrPd_2Ge_2$ superconductor in a dilution refrigerator down to $T = 60$ mK and in magnetic fields up to $H_{dc} = 1$ T by using a tunnel diode resonator. The London penetration depth λ saturates exponentially approaching $T \to 0$ indicating fully gapped superconductivity. The thermodynamic Rutgers formula was used to estimate $\lambda(0) = 426 \pm 60$ nm which was used to calculate the superfluid density, $\rho_s(T) = \lambda^2(0)/\lambda^2(T)$. Analysis of $\rho_s(T)$ in the full temperature range shows that it is best described by a single-gap behavior, perhaps with somewhat stronger coupling. In a magnetic field, the measured penetration depth is given by the Campbell penetration depth which was used to calculate the theoretical critical current density j_c. For $H \leqslant 0.45$ T, the strongest pinning is achieved not at the lowest, but at some intermediate temperature, probably due to matching effect between temperature-dependent coherence length and relevant pinning length scale. Finally, we find compelling evidence for surface superconductivity. Combining all measurements, the entire H-T phase diagram of $SrPd_2Ge_2$ is constructed with an estimated $H_{c2}(0) = 0.4817$ T.

DOI: 10.1103/PhysRevB.87.094515 PACS number(s): 74.25.Ha, 74.25.Sv, 74.25.Wx

I. INTRODUCTION

Superconductivity in the tetragonal $ThCr_2Si_2$-type $SrPd_2Ge_2$ was discovered first in polycrystalline samples[1] and later in single crystals[2] with the superconducting phase transition temperature (T_c) at 3.0 and 2.7 K, respectively. The upper critical field (H_{c2}) was estimated to be 4920 Oe at $T = 0$ by using Helfand-Werthamer (HW) theory[3] based on the experimental data obtained only down to $T = 0.7T_c$.[2] It has been found that T_c and H_{c2} can be slightly increased by chemical doping.[4] The London penetration depth and coherence length were reported to be $\lambda(0) = 566$ nm and $\xi(0) = 21$ nm (Ref. 5) and $\lambda(0) = 345 \pm 30$ nm $\xi(0) = 25.6 \pm 0.5$ nm.[6] These values give the Ginzburg-Landau parameter of $\kappa = 27$ (Ref. 5) and $\kappa = 13.5$ (Ref. 6), which makes $SrPd_2Ge_2$ a strong type-II superconductor. Furthermore, thermodynamic[2] and tunneling spectroscopy measurements are consistent with a strong-coupling s-wave Bardeen-Cooper-Schrieffer (BCS) superconductor with the zero-temperature value of the superconducting gap of $\Delta_0 \approx 2k_BT_c$,[5,6]—slightly higher but not far from the weak-coupling value of 1.76.

This superconductor is interesting particularly because of compositional similarity to the isostructural Fe-and Ni-pnictide superconductors with comparable T_c such as KFe_2As_2, $BaNi_2As_2$, and $SrNi_2P_2$. Although there is strong experimental evidence for nodal superconductivity in KFe_2As_2 (Refs. 7 and 8), the Ni-based compounds have been shown to be fully gapped by thermodynamic and thermal transport measurements.[9,10] This naturally prompts the question: what is the structure of a superconducting gap in $SrPd_2Ge_2$? So far, not much work has been done on $SrPd_2Ge_2$ in this direction. Tunneling spectroscopy between $0.17T_c$ and T_c is consistent with a single, isotropic gap superconductor.[5] However, the thermodynamic, thermal transport, and penetration depth measurements down to much lower temperatures are necessary to provide objective conclusions regarding the gap symmetry in $SrPd_2Ge_2$.

The magnetic penetration depth is among the most useful probes to explore the superconducting state.[11] In zero external magnetic field, this represents the London penetration depth. If measured with sufficient accuracy and down to low enough temperatures, it can be used to understand the angular variation of the superconducting gap on the Fermi surface.[11,12] In the presence of vortices, the magnetic field penetration includes contribution of the Campbell penetration depth which depends on the elastic properties of vortex lattice and is linked directly to the critical current density.[13] There has been only limited work performed in the mixed state of $SrPd_2Ge_2$[6,14] and no studies of the critical current density over the full temperature and field range.

In this article we report precision tunnel diode resonator measurements of the magnetic penetration depth $\lambda_m(T)$ in a single crystal of $SrPd_2Ge_2$ ($T_c = 2.7$ K) performed in a dilution refrigerator with temperatures down to $T \approx 0.02T_c$ and in magnetic fields up to 1 T $\approx 2H_{c2}(0)$. The low-temperature variation of the London penetration depth, $\Delta\lambda(T)$, clearly shows exponential saturation. The thermodynamic Rutgers formula was used to estimate $\lambda(0) = 426 \pm 60$ nm which was used to calculate the superfluid density, $\rho_s(T) = \lambda^2(0)/\lambda^2(T)$. Analysis of $\rho_s(T)$ in the full temperature range shows that it is best described by a single-gap behavior, perhaps with somewhat strong coupling. The upper critical field, $H_{c2}(0) = 0.4817$ T was determined by the HW theory from the field sweeps at different temperatures down to $0.02T_c$. In finite magnetic fields, $H < H_{c2}(0)$, the Campbell penetration depth $\lambda_C(T,H)$ shows a minimum at an intermediate temperature (rather than at the lowest temperature) which indicates nonmonotonic variation of the theoretical critical current (j_c) calculated from $\lambda_C(T,H)$. Additional diamagnetic response detected above $H_{c2}(T)$ is consistent with surface superconductivity with $H_{c3}(T) = 1.695H_{c2}(T)$.[15]

II. EXPERIMENT

Single crystals of $SrPd_2Ge_2$ were grown using a self-flux method as described in Ref. 2. The magnetic penetration depth

was measured in a dilution refrigerator by using a tunnel diode resonator (TDR) technique (for review, see Ref. 11). The sample with dimensions $(0.51 \times 0.70 \times 0.04)$ mm^3 with the shortest direction being along the c axis was mounted on a sapphire rod and inserted into a 2-mm-inner-diameter copper coil that produces rf excitation field with empty-resonator frequency of 17 MHz with amplitude $H_{ac} \sim 20$ mOe, much smaller than H_{c1} of typical conventional superconductors. Measurements of the in-plane magnetic penetration depth were done with both H_{dc} and $H_{ac} \| c$ axis. The shift of the resonant frequency (in cgs units), $\Delta f(T) = -G4\pi\chi(T)$, where $\chi(T)$ is the differential magnetic susceptibility, $G = f_0 V_s / 2V_c(1 - N)$ is a constant, N is the demagnetization factor, V_s is the sample volume, and V_c is the coil volume. The constant G was determined from the full frequency change by physically pulling the sample out of the coil. With the characteristic sample size R, $4\pi\chi = (\lambda/R)\tanh(R/\lambda) - 1$, from which $\Delta\lambda$ can be obtained.[11,16]

III. RESULTS AND DISCUSSION

A. London penetration depth

Figure 1 shows temperature variation of the in-plane London penetration depth, $\Delta\lambda(T)$, measured in a single crystal of $SrPd_2Ge_2$ superconductor which exhibits a very sharp superconducting phase transition at $T_c = 2.7$ K as shown in the inset, indicating a high quality, homogeneous sample. In the main panel, $\Delta\lambda(T)$ is shown with temperatures up to about $0.67T_c$. The saturation in $T \to 0$ limit and almost flat temperature dependence, $\Delta\lambda(T_c/3) < 10$ nm, indicate fully gapped superconductivity. Experimental $\Delta\lambda(T)$ is best fit to a power-law function, $\Delta\lambda(T) = AT^n$, with the exponent of $n = 2.7 \pm 0.1$ and prefactor of $A = 12.2 \pm 0.4$ nm/K.[2,7] The fitting curve is shown by the red solid line. A power-law

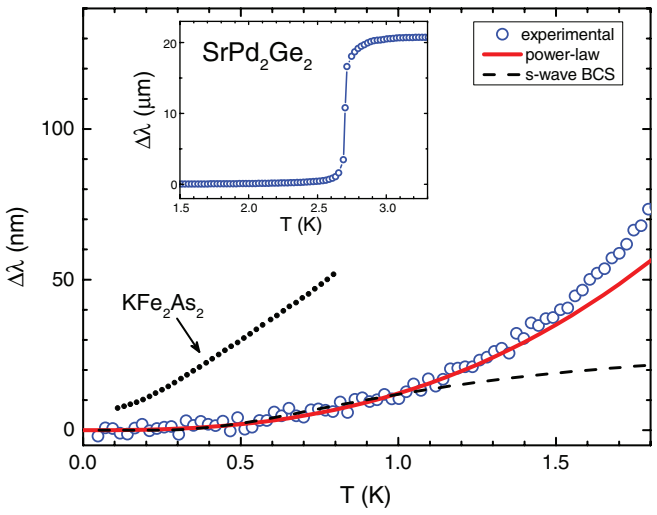

FIG. 1. (Color online) In-plane London penetration depth in a single crystal of $SrPd_2Ge_2$. Main panel: Open circles represent experimental data. Solid and dashed lines show power-law and BCS (single-gap s-wave) low-temperature fits. Dotted line shows the data for KFe_2As_2 taken from Ref. 7 for comparison. Inset: London penetration depth for temperatures between 1.5 K and 3.3 K demonstrating a sharp transition at $T_c = 2.7$ K.

function with such a high exponent has very weak variation at low temperatures, indistinguishable from the exponential behavior which is predicted for a full superconducting gap. In fact, the BCS low-temperature form, $\Delta\lambda(T) = \lambda(0)\sqrt{\pi\Delta_0/2k_BT}\exp(-\Delta_0/k_BT)$, where Δ_0 is the maximum gap value at $T = 0$, fits the data equally well for $T < T_c/3$ where it is expected to be valid. However, the best fitting is achieved with $\lambda(0) = 50$ nm and $\Delta_0 = 0.74k_BT_c$. The latter is impossible in the single-gap clean limit where $\Delta_0 \approx 1.76k_BT_c$ is expected. The value of $\lambda(0)$ is also much smaller than the reported value of 566 nm.[5] Similar low-temperature features can be seen in two-band superconductors such as MgB_2,[17] 2H-$NbSe_2$,[18] $Lu_2Fe_3Si_5$,[19] and more recently LiFeAs.[20] However, as we show below, analysis of the superfluid density in the full temperature range is inconsistent with a two-gap clean limit behavior. Instead, it is more likely that we are dealing with moderate pair-breaking scattering (maybe due to well-known magnetic impurities in Pd) which results in a finite density of states inside the gap. We also point out that total temperature variation of London penetration depth up to $T_c/3$ in $SrPd_2Ge_2$ is much smaller than in a known nodal superconductor with similar T_c, KFe_2As_2,[7] see Fig. 1. This difference indicates a difference in the density of quasi-particle excitations due to a difference in the nodal gap structure.

For a metallic sample, the measured penetration depth above T_c is determined either by the skin depth δ or sample size. In the case of skin depth limiting, the value of $\lambda(T > T_c)$ shown in the inset of Fig. 1 is one-half of the actual skin depth.[21] Therefore, we can estimate normal-state resistivity from the measurements using $\rho = (2\pi\omega/c^2)\delta^2$.[20] For $SrPd_2Ge_2$ with $\omega/2\pi = f_0 = 17$ MHz and $\delta/2 \approx 20$ μm, the calculated resistivity is approximately 12 $\mu\Omega$ cm which is much less than the experimental value of 68 $\mu\Omega$ cm.[2] Therefore, we conclude that our measurements are taken in a sample-size limited regime. Using the same equation, the estimated skin depth is 0.10 mm which means the rf field penetration is comparable to the dimensions of the sample.

Finally, we note that the data exhibit a smooth transition from superconducting penetration depth to the normal state between $T = T_c$ and $T^* \approx 3.0$ K, which has also been seen in transport measurement.[2] Interestingly, $T^* = 3$ K is the onset of superconductivity observed in polycrystalline samples.[1] A similar feature has also been observed in a related superconductor $BaNi_2As_2$.[22] Perhaps this feature requires further study.

B. Superfluid density

While the low-temperature behavior is important for characterization of the gap minima, the superconducting gap can be probed at all energies by the analysis of the superfluid density, $\rho_s(T) = \lambda^2(0)/\lambda^2(T)$, in the entire temperature range.[12] However, determination of ρ_s requires knowledge of the absolute value of $\lambda(0)$ which does not come from our measurements. In $SrPd_2Ge_2$, $\lambda(0) = 40$ nm was suggested from measured band structure parameters in the clean limit,[5] which leads to $\lambda(0) = 566$ nm in the dirty limit. Also, $\lambda(0) \approx 390$ nm was estimated from the upper critical field measurements,[2] and $\lambda(0) = 345 \pm 5$ nm from first field penetration value.[6] The variation of the literature values is quite significant and

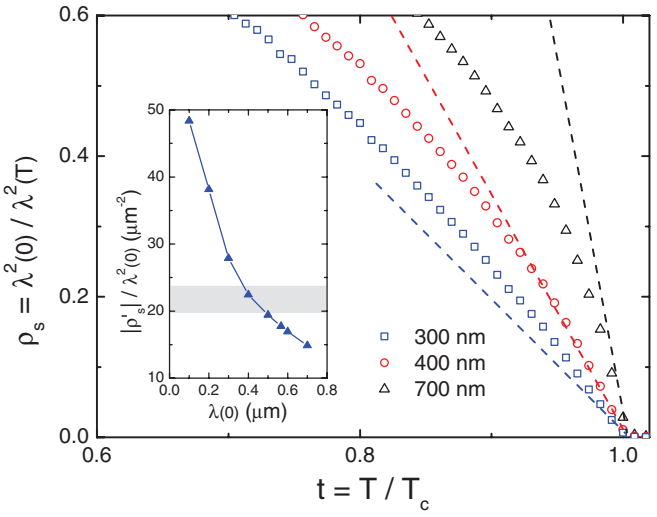

FIG. 2. (Color online) Main panel: Calculated superfluid density ρ_s with various $\lambda(0)$'s. The slope of dashed lines was determined with ΔC_p and $|dH_{c2}/dT|_{T_c}$ using the Rutgers formula as described in the text. Inset: Variation of $|\partial\rho_s/\partial t|_{T_c}/\lambda^2(0)$ with varying $\lambda(0)$. Here ρ_s' was determined from the experimental data. The gray band is a theoretical estimate with 5% hypothetical error in ΔC_p and $|dH_{c2}/dT|_{T_c}$.

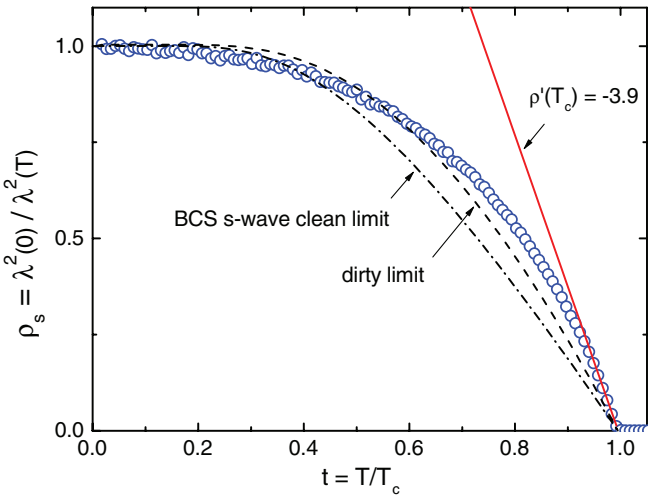

FIG. 3. (Color online) Calculated superfluid density, $\rho_s(T) = \lambda^2(0)/\lambda^2(T)$ using $\lambda(0) = 426$ nm. Open circles represent the experimental data. The dash-dotted and dashed lines represent single-gap weak-coupling s-wave BCS superconductor in clean and dirty limit, respectively.

below we use, thermodynamic approach based on the Rutgers formula,[23] relating various superconducting state parameters at T_c. This formula was adapted for the use with the superfluid density by Kogan[24] as briefly described here. In the Ginzburg-Landau regime, i.e. near T_c, it is straightforward to show that

$$\left|\frac{\partial\rho_s}{\partial t}\right|_{T_c} = \frac{16\pi^2\lambda^2(0)}{\phi_0|\partial H_{c2}/\partial T|_{T_c}}\Delta C_p, \qquad (1)$$

where $\phi_0 = 2.07\times10^{-7}$ G cm^2 is a flux quantum and $|\partial H_{c2}/\partial T|_{T_c} = 0.26$ T/K is determined experimentally (see Fig. 8 below). Specific-heat jump $\Delta C_p = 7381$ erg/cm^3 K is taken from Ref. 4. Applying these thermodynamic values suggests $|\partial\rho/\partial t|_{T_c}/\lambda^2(0) = 21.7\ \mu$m^{-2} where $t = T/T_c$ is the reduced temperature. This quantity can be compared with the actual slope of calculated $\rho_s(t)$ with various $\lambda(0)$ at T_c as shown in Fig. 2. In the main panel of Fig. 2, the open symbols represent the superfluid density calculated using $\lambda(0) = 300, 400$, and 700 nm for triangles, circles, and squares, respectively. The dashed lines are determined with the slope calculated by Eq. (1) for the three values of $\lambda(0)$ quoted above. The line for $\lambda(0) = 400$ nm shows very good agreement with calculated ρ_s while the line for $\lambda(0) = 300$ nm significantly underestimates, and the one for $\lambda(0) = 700$ nm overestimates $\rho_s(T)$. This procedure can be repeated with various values of $\lambda(0)$. The results are summarized in the inset where the solid triangles represent experimental slopes obtained by fitting experimental data near T_c to a linear function. The gray horizontal band represents the theoretical value of $|\partial\rho/\partial t|_{T_c}/\lambda^2(0) = 21.7\pm2.2\ \mu$m^{-2} determined with a 5% hypothetical error in $|\partial H_{c2}/\partial T|_{T_c}$ and ΔC_p. In this way, $\lambda(0)$ can be determined at the intersection of the theoretical line and experimental results, which provides that $\lambda(0) = 426\pm60$ nm that lies between the literature values. With this value, the slope of ρ_s at T_c is determined to be -3.9.

The superfluid density calculated with $\lambda(0) = 426$ nm is shown in Fig. 3. The dash-dotted and dashed lines show the expectation for the clean and dirty limits of a single-gap BCS superconductor in the weak-coupling limit, respectively. An attempt to use a two-gap (clean) γ model[25] in the full-temperature range converges to a single-gap limit with $\Delta(0)/k_BT_c = 2.2$. Therefore, the superconducting gap of $SrPd_2Ge_2$ is best represented by a single-gap s-wave function, perhaps with somewhat enhanced coupling strength. It was noted previously that the shape of $\rho_s(T)$ is close to a nonlocal-limiting case, expected in type-I superconductors such as aluminum and cadmium.[26] A similar argument was made in the work by Kim *et al.* in which $SrPd_2Ge_2$ appeared to be type I according to the intrinsic electronic structure despite the fact that experimental $\xi(0)$ and $\lambda(0)$ values put it in a strong type-II regime.[5] In any case, our study confirms that simple analysis with an isotropic Fermi surface is not sufficient and, perhaps, the results could be explained by taking into account a realistic band structure. We can, however, conclude that the superconducting gap of $SrPd_2As_2$ does not have nodes.

C. Campbell penetration depth

Figure 4(a) shows magnetic penetration depth $\Delta\lambda_m(T,H)$ as a function of temperature and magnetic field measured after cooling without magnetic field to target low temperature and then applying a dc magnetic field of indicated amplitude [zero-field cooled (ZFC): solid lines] and upon cooling in field (FC: dashed lines). Increasing dc magnetic field not only suppresses the superconducting phase transition and diamagnetic shielding, but also induces another diamagnetic phase between the normal state and apparent bulk superconductivity. This feature appears much clearer above $H = 0.2$ T and persists at least up to $H = 0.6$ T which is far greater than the upper critical field of the bulk superconductivity. This feature can hardly

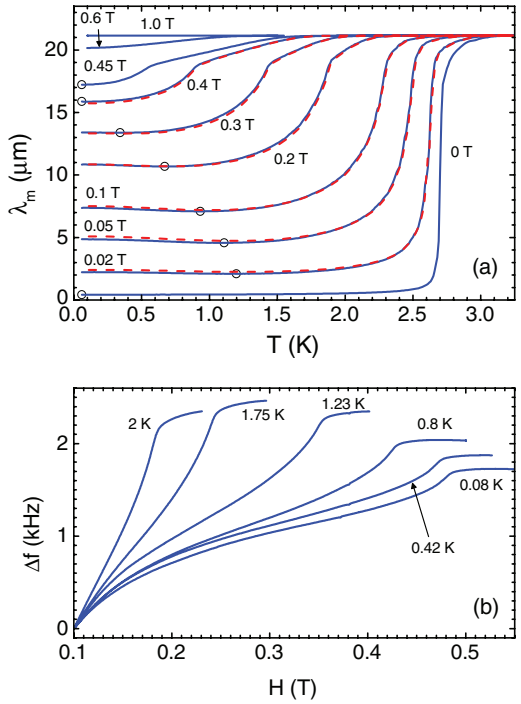

FIG. 4. (Color online) (a) Zero-field-cooled (ZFC) and field-cooled (FC) in-plane magnetic penetration depth measured in a single crystal of $SrPd_2Ge_2$ shown by solid and dashed lines, respectively. Open circles mark the minimum in $\lambda_m(T)$ in each magnetic field. (b) Magnetic field sweeps at fixed temperatures.

be understood with sample inhomogeneity or second phases since they both should affect the measurements in zero field. Systematic tracking of this feature reveals its possible connection to surface superconductivity, which will be discussed later together with the general H-T phase diagram. In addition to temperature sweeps at fixed dc magnetic fields, magnetic field sweeps at different fixed temperatures were performed, and superconducting transitions are clearly detected as shown in Fig. 4(b). The determined bulk $H_{c2}(T)$ is consistent with $T_c(H)$ determined from the temperature scans. We note that the anomaly above $H_{c2}(T)$ was not detected in the field sweep measurements.

Another unusual experimental observation is apparently the nonmonotonic temperature variation of $\Delta\lambda_m(T,H)$ for $0.02\ \mathrm{T} \leqslant H \leqslant 0.4\ \mathrm{T}$ in both ZFC and FC data. The minima of $\Delta\lambda_m(T,H)$ are marked by open circles for clarity in Fig. 4(a), and the locations of these minima are nearly the same for both ZFC and FC data. This feature is too shallow to be due to paramagnetic impurities (in which case it should be most pronounced at $H = 0$).[27] We suggest that this behavior is caused by the size matching of the temperature-dependent coherence length and relevant pinning centers. Furthermore, we observed the inversion of diamagnetic screening between ZFC and FC runs at about $H = 0.2$ T. The only way to obtain a difference between FC and ZFC experiments in ac response is to assume a nonparabolic pinning potential[28] and our results would indicate that the effective pinning potential shape is strongly field and temperature dependent. Conventional superconductors, like $YbSb_2$ (Ref. 29) do not exhibit such upturns in a magnetic field.

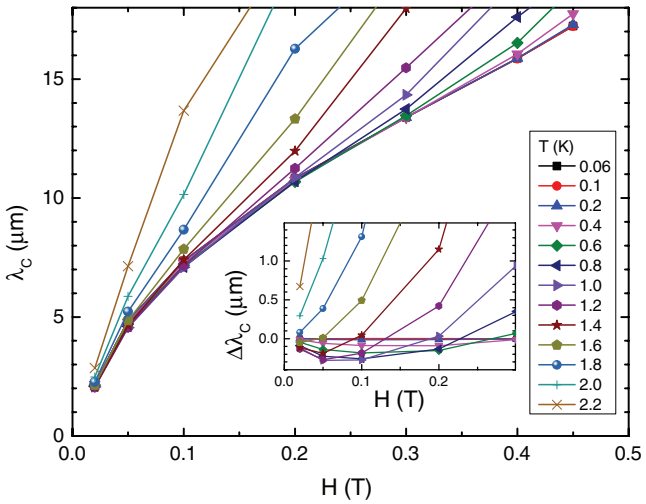

FIG. 5. (Color online) Isothermal Campbell penetration depth as function of a dc magnetic field calculated from the data of Fig. 4(a). Inset: $\Delta\lambda_C(T,H) = \lambda_C(0.06\ \mathrm{K},H) - \lambda_C(T,H)$ is displayed to show nonmonotonic behavior.

In the approximation of a linear elastic response of a vortex lattice to a small-amplitude ac perturbation (which is the case here), the total magnetic penetration depth can be expressed as a sum of Meissner and vortex contributions, which are represented by the London and Campbell penetration depths, respectively, $\lambda_m^2 = \lambda^2 + \lambda_C^2$.[13,30,31] Since we know λ from the measurements in zero field, we can readily calculate λ_C. At first glance, the field dependence of the Campbell penetration depth, shown in Fig. 5, appears sublinear, $\sqrt{H}$, as expected in conventional superconductors. However, nonmonotonic behavior is revealed upon closer inspection as shown in the inset. This nonmonotonic behavior at low fields originates from nonmonotonic temperature dependence of λ_m discussed above.

D. Theoretical critical current

We distinguish theoretical critical current, which is a parameter entering the simple expression for the Campbell penetration depth, $\frac{4\pi}{c} j_c = r_p \phi_0 / \lambda_C^2$ from the actual critical current that is affected by intervortex interactions and from the measured critical (persistent) current that is further affected by magnetic relaxation. Here r_p is a characteristic radius of the pinning potential. We assume the r_p to be equal to the coherence length $\xi(T) = \sqrt{\phi_0 / 2\pi H_{c2}(T)}$. Obtained theoretical critical current density is shown in Fig. 6(a) as function of temperature at different fields and in Fig. 6(b) as a function of applied fields at different temperatures. The critical current is nonmonotonic as a function of temperature, showing maximum at the intermediate temperatures. We attribute this to the matching between temperature-dependent coherence length and pinning landscape. This assertion is plausible given monotonic behavior of the critical current versus field where the variation of the coherence length is much weaker.[32] Comparison with the previous works also reaffirms that we are dealing with the upper theoretical estimate of the critical current, approximately four times larger than evaluated from the magnetic measurements.[14] On the other

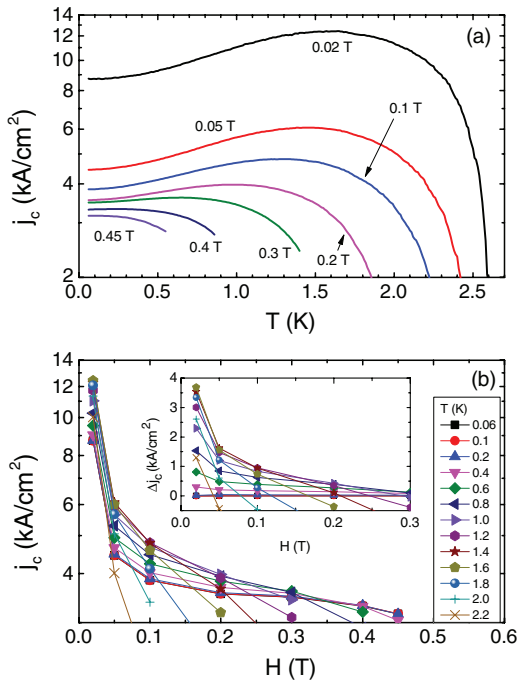

FIG. 6. (Color online) Calculated theoretical critical current (a) as a function of temperature in different magnetic fields and (b) as a function of magnetic field at fixed temperatures. Inset in (b) displays $\Delta j_c(T,H) = j_c(T,H) - j_c(0.06\text{K},H)$ to show the maximum j_c being at a intermediate temperature.

hand, direct comparison with our data, Fig. 8, shows that the line of the maximum current density found in this work is not an extension of the irreversibility line found in Ref. 14 and probably represents a crossover in the pinning mechanism reflected in the change of the effective pinning potential.

Unfortunately literature data are only available for higher temperatures, above $T = 2$ K, and for weak fields less than $H = 0.1$ T, so we do not know whether the nonmonotonic behavior of $j_c(T)$ propagates to the relaxed persistent current density. Furthermore, our evaluation of the coherence length, $\xi(T)$ (right axis in Fig. 7), allows experimental determination of the temperature-dependent Ginzburg-Landau parameter, $\kappa(T) = \lambda(T)/\xi(T)$, shown in Fig. 7 (left axis). The result is compared with the Gor'kov theory[33] where temperature correction is introduced as $A_G(T) = \kappa(T)/\kappa(T_c)$. The trend is correct, but the magnitude of the variation is smaller then the observed. If we attempt to rescale the Gor'kov's result, the best agreement at the intermediate temperatures is achieved with $\kappa(T) = \kappa(T_c)[2.6A_G(T) - 1.6]$. Perhaps a better agreement could be achieved with a realistic band structure.

E. *H-T* phase diagram

Finally, a H-T phase diagram is established based on the measured $\Delta\lambda_m(T,H)$ as shown in Fig. 8. Open and solid circles represent bulk superconducting phase transitions determined from temperature- and field-sweep measurements, respectively. The upper critical field was determined at the maximum of $d\Delta\lambda/dT$ and $d\Delta f/dH$ in temperature- and field-sweep experiments in Fig. 4, respectively. The red solid line through the symbols is the HW fit[3] with $H_{c2}(0) = 0.4817$ T.

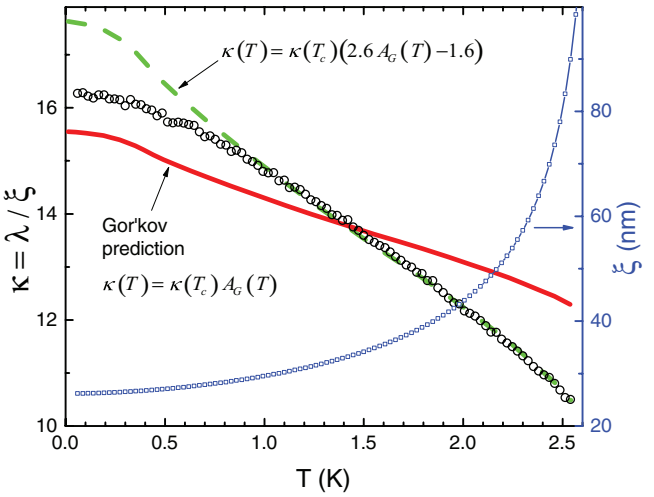

FIG. 7. (Color online) Calculated Ginzburg-Landau parameter, $\kappa(T) = \lambda(T)/\xi(T)$ (symbols, left axis) compared to the Gor'kov prediction, $\kappa(T) = \kappa(T_c) A_G(T)$ (solid line) and to modified to best fit the data expression, $\kappa(T) = \kappa(T_c)(2.6A_G(T) - 1.6)$ (dashed line). Right axis shows estimated coherence length.

This value was determined with the experimental data down to $0.02T_c$ in our study, and it is very close to the estimated value $H_{c2}(0) = 0.4920$ T in Ref. 2 only with the the slope at T_c by using the same theory. This is a good indication that $H_{c2}(T)$ of $SrPd_2Ge_2$ is orbital limited.

The additional diamagnetic phase between bulk T_c and normal state detected in temperature sweeps is marked by open squares. This phase transition is clearest in magnetic fields between 0.2 and 0.6 T. A linear fit through these squares

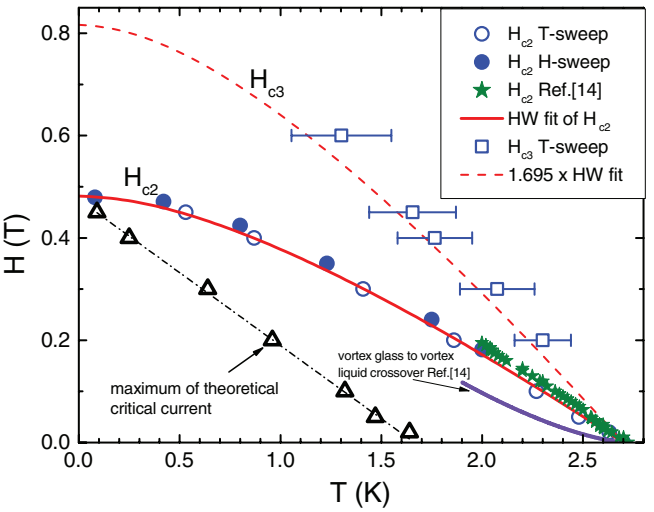

FIG. 8. (Color online) H-T phase diagram of $SrPd_2Ge_2$. Open and solid circles represent bulk superconducting transition, $H_{c2}(T)$, determined by temperature and field sweeps, respectively. Red solid line is fitting over experimental $H_{c2}(T)$ using the HW theory. Open squares indicate the temperatures where diamagnetic response was detected above bulk T_c. Red dashed line represents $H_{c3} = 1.695H_{c2}(T)$. Open triangles with black dash-dotted linear fit line show maximum of the pinning. For comparison, we include the data for H_{c2} (green stars) and a crossover from vortex liquid to vortex glass phase (violet solid line) from Ref. 14.

extrapolates down to almost $H_{c2}(T_c)$ and up to 1 T where the diamagnetic phase was not seen. It is well known that surface superconductivity boundary is given by $H_{c3}(T) = 1.695H_{c2}(T)$.[15] This curve fits well the diamagnetic feature observed in our experiments, so it makes sense to assign it to surface superconductivity.

The region of the strongest pinning, where the theoretical critical current is maximum, is marked in Fig. 8 with solid traingles with linear fit dashed-dotted line. This region lies deep inside the superconducting state and is probably due to the matching effect. For comparison, we include the data for H_{c2} (green stars) and for a crossover from vortex liquid to vortex glass phase (violet solid line), both estimated from the magnetization measurements.[14] The upper critical field is in a good agreement with our data. The liquid-glass crossover line, on the other hand, does not extrapolate to the line of the strong pinning found in our measurements (although there is no overlapping temperature interval). This indicates that the maximum theoretical critical current line is not an extension of the irreversibility line and represents a different crossover in the pinning mechanism reflected in the nonmonotonic change in the shape of the pinning potential.

IV. SUMMARY

Temperature- and magnetic-field-dependent penetration depth was measured in single crystals of $SrPd_2Ge_2$ superconductor by using a tunnel diode resonator technique. For $H = 0$, the London penetration depth saturates at low temperatures indicating a fully gapped superconductivity in $SrPd_2Ge_2$. The calculated superfluid density is best described by a single-gap s-wave superconductor, perhaps slightly on the stronger coupling side. The $H_{c2}(T)$ was measured down to $0.02T_c$ and could be well described by the HW theory with $H_{c2}(0) = 0.4817$ T and is clearly limited by the orbital depairing. In the magnetic fields between 0.2 and 0.6 T, another diamagnetic phase different from bulk superconductivity is clearly seen, and this phase line is consistent with the surface superconductivity bound by the third critical field, $H_{c3} = 1.695H_{c2}$. The Campbell penetration depth and the theoretical critical current density both exhibit nonmonotonic behavior with the strongest pinning at intermediate temperatures. We assign maximum pinning to matching effects between the temperature-dependent coherence length and the relevant pinning landscape length scale.

ACKNOWLEDGMENTS

R.P., M.A.T., and H.K. thank V. G. Kogan for insightful comments and the suggestion to use the thermodynamic Rutgers formula for analysis of the superfluid density. H.K. and N.H.S. thank J. Kim for useful discussions. The work at Ames was supported by the US Department of Energy, Office of Basic Energy Sciences, Division of Materials Sciences and Engineering under Contract No. DE-AC02-07CH11358. The work at GIST was supported by the Ministry of Education, Science and Technology of the Republic of Korea (Grant No. 2011-0028736).

*hyunsoo@iastate.edu
†nakheon@gmail.com
‡chobk@gist.ac.kr
§tanatar@ameslab.gov
|Corresponding author: prozorov@ameslab.gov

[1]H. Fujii and A. Sato, Phys. Rev. B **79**, 224522 (2009).
[2]N. H. Sung, J.-S. Rhyee, and B. K. Cho, Phys. Rev. B **83**, 094511 (2011).
[3]E. Helfand and N. R. Werthamer, Phys. Rev. **147**, 288 (1966).
[4]N. H. Sung, C. J. Roh, B. Y. Kang, and B. K. Cho, J. Appl. Phys. **111**, 07E117 (2012).
[5]T. K. Kim, A. N. Yaresko, V. B. Zabolotnyy, A. A. Kordyuk, D. V. Evtushinsky, N. H. Sung, B. K. Cho, T. Samuely, P. Szabó, J. G. Rodrigo, J. T. Park, D. S. Inosov, P. Samuely, B. Büchner, and S. V. Borisenko, Phys. Rev. B **85**, 014520 (2012).
[6]T. Samuely, P. Szabó, Z. Pribulovó, N. H. Sung, B. K. Cho, T. Klein, V. Cambel, J. G. Rodrigo, and P. Samuely, Supercond. Sci. Technol. **26**, 015010 (2013).
[7]K. Hashimoto, A. Serafin, S. Tonegawa, R. Katsumata, R. Okazaki, T. Saito, H. Fukazawa, Y. Kohori, K. Kihou, C. H. Lee, A. Iyo, H. Eisaki, H. Ikeda, Y. Matsuda, A. Carrington, and T. Shibauchi, Phys. Rev. B **82**, 014526 (2010).
[8]J.-P. Reid, M. A. Tanatar, A. Juneau-Fecteau, R. T. Gordon, S. R. de Cotret, N. Doiron-Leyraud, T. Saito, H. Fukazawa, Y. Kohori, K. Kihou, C. H. Lee, A. Iyo, H. Eisaki, R. Prozorov, and L. Taillefer, Phys. Rev. Lett. **109**, 087001 (2012).
[9]N. Kurita, F. Ronning, Y. Tokiwa, E. D. Bauer, A. Subedi, D. J. Singh, J. D. Thompson, and R. Movshovich, Phys. Rev. Lett. **102**, 147004 (2009).
[10]N. Kurita, F. Ronning, C. F. Miclea, E. D. Bauer, K. Gofryk, J. D. Thompson, and R. Movshovich, Phys. Rev. B **83**, 094527 (2011).
[11]R. Prozorov and R. W. Giannetta, Supercond. Sci. Technol. **19**, R41 (2006).
[12]R. Prozorov and V. G. Kogan, Rep. Prog. Phys. **74**, 124505 (2011).
[13]E. H. Brandt, Rep. Prog. Phys. **58**, 1465 (1995).
[14]N. H. Sung, Y. J. Jo, and B. K. Cho, Supercond. Sci. Technol. **25**, 075002 (2012).
[15]M. Tinkham, *Introduction to Superconductivity*, 2nd ed. (Dover, New York, 2004).
[16]R. Prozorov, R. W. Giannetta, A. Carrington, and F. M. Araujo-Moreira, Phys. Rev. B **62**, 115 (2000).
[17]J. D. Fletcher, A. Carrington, O. J. Taylor, S. M. Kazakov, and J. Karpinski, Phys. Rev. Lett. **95**, 097005 (2005).
[18]J. D. Fletcher, A. Carrington, P. Diener, P. Rodiere, J. P. Brison, R. Prozorov, T. Olheiser, and R. W. Giannetta, Phys. Rev. Lett. **98**, 057003 (2007).
[19]R. T. Gordon, M. D. Vannette, C. Martin, Y. Nakajima, T. Tamegai, and R. Prozorov, Phys. Rev. B **78**, 024514 (2008).
[20]H. Kim, M. A. Tanatar, Y. J. Song, Y. S. Kwon, and R. Prozorov, Phys. Rev. B **83**, 100502 (2011).

[21]E. M. Lifshitz, L. D. Landau, and L. P. Pitaevskii, *Electrodynamics of Continuous Media*, 2nd ed. (Butterworth-Heinemann, London, 1984).
[22]F. Ronning, N. Kurita, E. D. Bauer, B. L. Scott, T. Park, T. Klimczuk, R. Movshovich, and J. D. Thompson, J. Phys.: Condens. Matter **20**, 342203 (2008).
[23]A. J. Rutgers, Physica **1**, 1055 (1934).
[24]Hyunsoo Kim, K. Cho, M. A. Tanatar, R. Prozorov, and V. G. Kogan (in preparation).
[25]V. G. Kogan, C. Martin, and R. Prozorov, Phys. Rev. B **80**, 014507 (2009).
[26]I. Bonalde, B. D. Yanoff, M. B. Salamon, and E. E. M. Chia, Phys. Rev. B **67**, 012506 (2003).
[27]J. R. Cooper, Phys. Rev. B **54**, R3753 (1996).
[28]R. Prozorov, R. W. Giannetta, N. Kameda, T. Tamegai, J. A. Schlueter, and P. Fournier, Phys. Rev. B **67**, 184501 (2003).
[29]L. L. Zhao, S. Lausberg, H. Kim, M. A. Tanatar, M. Brando, R. Prozorov, and E. Morosan, Phys. Rev. B **85**, 214526 (2012).
[30]A. M. Campbell, J. Phys. C **2**, 1492 (1969).
[31]A. M. Campbell, J. Phys. C **4**, 3186 (1971).
[32]V. G. Kogan, R. Prozorov, S. L. Bud'ko, P. C. Canfield, J. R. Thompson, J. Karpinski, N. D. Zhigadlo, and P. Miranovic, Phys. Rev. B **74**, 184521 (2006).
[33]L. P. Gor'kov, Sov. Phys. JETP **10**, 593 (1960).